JATIS Journal of Astronomical Telescopes, Instruments, and Systems

RESEARCH PAPER

Line Emission Mapper: an X-ray probe mission concept to study the cosmic ecosystems and the physics of galaxy formation

Daniel J. Patnaude,[a,*] Ralph P. Kraft,[a] Caroline Kilbourne,[b] Simon Bandler,[b] Akos Bogdan,[a] Renata Cumbee,[b] Megan Eckart,[c] Cecilia Garraffo,[a] Edmund Hodges-Kluck,[b] Richard Kelley,[b] Maxim Markevitch,[b] Anna Ogorzalek,[b,d] Paul Plucinsky,[a] Frederick Scott Porter,[b] John ZuHone,[a] Irina Zhuravleva,[e] Jeremy Drake,[a] Maurice Leutenegger,[b] Steve Kenyon,[b] Stephen Smith,[b] Will Zhang,[b] Steve DePalo,[b] Xiaoyi Li,[b] Nathan Williams,[b] Edward Amatucci,[b] Janice Houston,[a] Deme Apostolou,[a] Hugh Kanner,[a] Kathleen Coderre,[f] Isaac Hayden,[f] Kyle Martin,[f] Elizabeth Osborne,[f] Jeffery Olson,[f] Steven Ramm,[f] and Scott Richardson[f]

[a]Center for Astrophysics | Harvard and Smithsonian, Cambridge, Massachusetts, United States
[b]NASA - Goddard Space Flight Center, Greenbelt, Maryland, United States
[c]Lawrence Livermore National Laboratory, Livermore, California, United States
[d]The University of Maryland, College Park, Maryland, United States
[e]The University of Chicago, Department of Astronomy and Astrophysics, Chicago, Illinois, United States
[f]Lockheed Martin Space, Palo Alto, California, United States

ABSTRACT. In the 2020 Astrophysics Decadal Survey, the National Academies identified cosmic feedback and structure formation as a key question that should drive research in the upcoming decade. In response to this recommendation, NASA released a call for X-ray and IR probe-class missions, with a $1B cost cap. The line emission mapper (LEM) is a mission concept designed in response to this call. LEM is a single-instrument X-ray telescope that consists of a Wolter–Schwarzschild type I X-ray optic with a 4 m focal length, coupled with an X-ray microcalorimeter with a 30′ field of view (FoV), 15″ angular resolution, and 2.5 eV energy resolution [full-width half maximum (FWHM)], with a 1.3 eV FWHM energy resolution central subarray. The high throughput X-ray mirror combined with the large FoV and excellent energy resolution allows for efficient mapping of extended emission-line dominated astrophysical objects from megaparsecs to sub-pc scales to study cosmic ecosystems and unveil the physical drivers of galaxy formation.

Keywords: missions; optics; detectors

Paper 23085SS received Jul. 21, 2023; revised Oct. 20, 2023; accepted Oct. 23, 2023; published Nov. 14, 2023.

1 Introduction

The National Academies' 2020 Decadal Survey in Astronomy and Astrophysics (Astro2020) videntified "cosmic ecosystems" and "the drivers of galaxy growth" as themes for new discovery space in the coming decades.[1] In direct response to this charge, the line emission mapper (LEM) was conceived to provide new insight into the formation and evolution of structure in the Universe. LEM consists of a directed Principal Investigator-led science program focusing on

*Address all correspondence to Daniel Patnaude, dpatnaude@cfa.harvard.edu

structure formation at all scales, a general observer (GO) program, and an all-sky survey with a guest investigator program. LEM will provide unprecedented insight into the kinematics, thermodynamics, and chemistry of hot gas as it flows between galaxies, the circumgalactic medium (CGM), and the expansive intergalactic medium (IGM) and intra-cluster medium. LEM will provide the entire astrophysics community with a powerful new tool with capabilities that will vastly outperform all existing or planned X-ray observatories. With a 5-year mission lifetime, LEM will lead to new understandings about the workings of active galactic nuclei, compact objects, accretion physics, the impact of stellar activity on planetary formation and evolution, cosmology, the life and death of stars, the nature of dark matter, and insight into new physics at all scales.

LEM is configured as a single science instrument consisting of a Wolter–Schwarzchild (WS) X-ray optic with a 10″ half power diameter (HPD) coupled with an X-ray microcalorimeter with a $\sim 30' \times 30'$ field of view (FoV). The LEM X-ray microcalorimeter (LMS) has 15″ pixels that are paired with the X-ray optic to ensure that bright X-ray sources will be contained within one or two pixels, so that they may be discriminated from the faint, diffuse background emission. When combined with the 4 m focal length, this design is optimized for surveying diffuse X-ray emission, while also enabling observations of bright, galactic sources. The LMS consists of a 7′ diameter central array with 1.3 eV full-width half maximum baseline energy resolution pixels, surrounded by a larger array of 2×2 pixel "hydras," four pixels coupled to a single transition edge sensor (TES) with 2.5 eV baseline resolution. All together, each 15″ LMS pixel will provide $E/\Delta E \sim 200$ to 2000 over the 0.2 to 1.9 keV bandpass. As mentioned above, by design, LEM is optimized for large-scale, low-surface-brightness, diffuse thermal X-ray emission in the Milky Way and across the Universe. Compared to Chandra and X-ray Multi-Mirror-Newton, LEM will be two orders of magnitude more sensitive to diffuse emission from hot gas in external galaxies and the IGM, which is seen through the bright screen of the Milky Way.

As LEM was conceived in direct response to the science priorities of the Astro2020 decadal survey,[1] it directly connects to NASA's astrophysics priorities. The importance of an X-ray probe was clearly identified as critical to addressing key questions in each of the three decadal science themes. The directed portion of LEM science is focused on the "cosmic ecosystems" theme. It was stated in the Astro2020 report that "this (feedback) profoundly multi-scale problem requires connecting galaxies from their central black holes... to their outer regions millions of light years from the center" (pp 1–8 of the Astro2020 decadal survey). LEM will allow us to understand the dynamical and thermodynamic state of the hot gas in galaxies from scales of parsecs (pc) to tens of megaparsecs (Mpc)—over seven orders of magnitude in length scale. The sub-panel on galaxies also clearly identified the need for a wide-FoV X-ray integral field unit (X-IFU) to address all science questions and its discovery area as well.

In this paper, we outline the LEM mission, presenting an overview of the mission concept, LEM science, and how LEM has been designed to address its core science program. We describe the key components of the mission but defer presentation of the finer details of the LMS to other contributions in this JATIS special section.[2–7] In Sec. 2, we describe the mission, including the spacecraft design, choice of orbit, and operational modes. Section 3 provides a broad overview of the LEM-directed science case, citing specific but non-exhaustive examples of the science which LEM will address. Finally, in Sec. 4, we discuss the key components of the LEM mission.

2 Mission Overview

LEM consists of a single X-ray instrument designed to probe key physics called out in the 2020 National Academies Decadal Survey in Astronomy and Astrophysics. The mission consists of a 1.5 m diameter 10″ HPD X-ray optic with a 4 m focal length, coupled to a $30' \times 30'$ X-ray microcalorimeter with 15″ pixels ($\lesssim$14 K pixels total). The baseline, current best estimate, and threshold requirements are listed in Table 1. (The baseline requirements are driven by the science requirements for the mission, while the threshold requirements represent the point at which the science goals cannot be met by the capabilities of the instrument.) The LEM focal plane array consists of an inner 7′ diameter array of 15″ pixels with 1.3 eV resolution, surrounded by a larger array of 2×2 pixel "hydras" with 2.5 eV resolution, filling out the 30′ diameter focal plane.

Table 1 LEM instrument requirements.

Requirement	Baseline	CBE	Threshold
Energy band (keV)	0.2 to 1.9	0.05 to 2.5	0.3 to 1.9
Energy resolution (eV)	—	—	—
Single TES inner array	1.3	1.2	2.0
Hybrid TES outer array	2.5	2.3	4.0
Effective area @ 0.5 keV (cm^2)	1200	1540	800
FoV (arcmin)	30	33	25
Angular resolution HPD (arcsec)	18	12	20
XMA allocation HPD (arcsec)	10	5.6	13
Detector background ($cts\,s^{-1}$ keV^{-1} FoV^{-1})	2	1	2

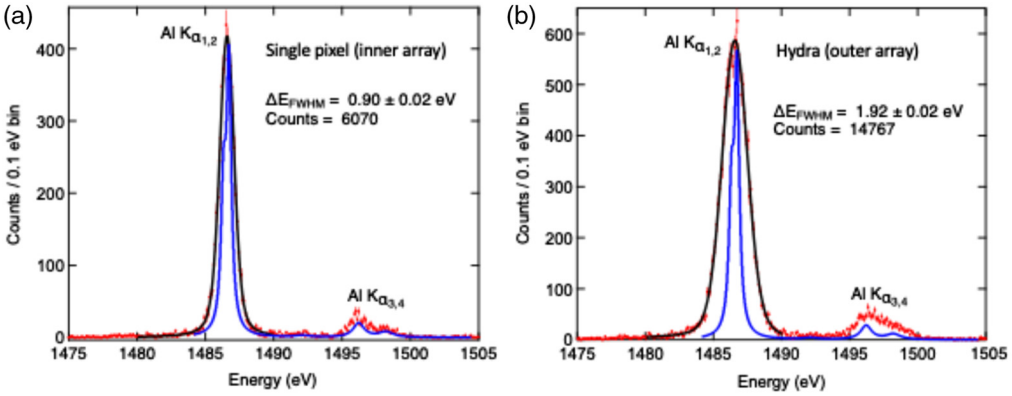

Fig. 1 (a) Single pixel spectral response for LEM inner array. (b) Spectral response of LEM 2×2 hydra pixel array.[8] In both panels, the data are shown in red, and the blue dotted line is the intrinsic width of the Al K$\alpha_{1,2}$ line, while the black curves represent a model fit to the data, including detector broadening. Consideration of the Al K$\alpha_{3,4}$ line is not included in the fit to the data.

The spectral performance of the single pixel and hydra arrays is shown in Fig. 1. The 1.3 to 2.5 eV energy resolution of the LEM X-ray microcalorimeter enables gas velocity measurements to 50 $km\,s^{-1}$.

The notional LEM satellite concept is shown in Fig. 2, with key requirements listed in Table 1. The "grasp," a product of the telescope effective area and detector FoV, allows for efficient mapping of diffuse, low surface brightness objects. As shown in Fig. 3, LEM will have a factor several times less area than Athena, but due to its large FoV, it will make up for this with the much larger grasp. Thus, LEM is optimally suited for mapping extended, diffuse emission efficiently. When the telescope grasp is combined with the energy resolution of the LMS, LEM will provide a multidimensional view of the Universe that is otherwise inaccessible to other existing or planned X-ray missions.

To maximize the scientific return of the mission, LEM will be placed in a quasi-halo orbit at the L1 Lagrange point, located between the Earth and the Sun. The choice of orbit is driven by the need for a low, stable, and well characterized background.[9] LEM will be able to observe all targets with a sun–satellite-object angle between 45 deg and 150 deg. This will allow for observations of solar system objects including Venus, the Moon, and the Earth. As shown in Fig. 4, over the course of a year the average visibility of a target in the ecliptic plane will be $\lesssim$60%, while all targets with ecliptic latitudes $>|46°|$ will be visible 100% of the time. Given the large fraction

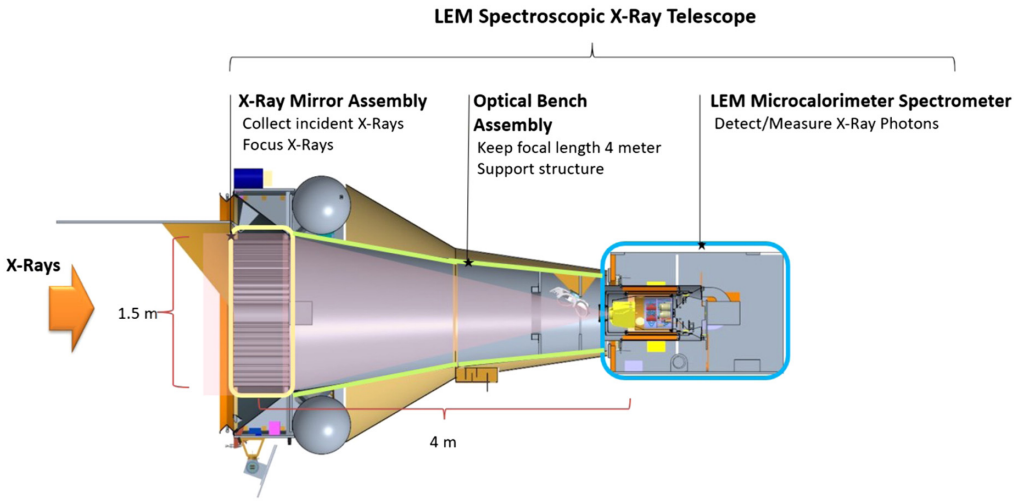

Fig. 2 LEM: the instrument consists of a 1.5 m diameter f/4 X-ray optic coupled to a $30' \times 30'$ FoV X-ray microcalorimeter with 1.3 to 2.5 eV energy resolution.

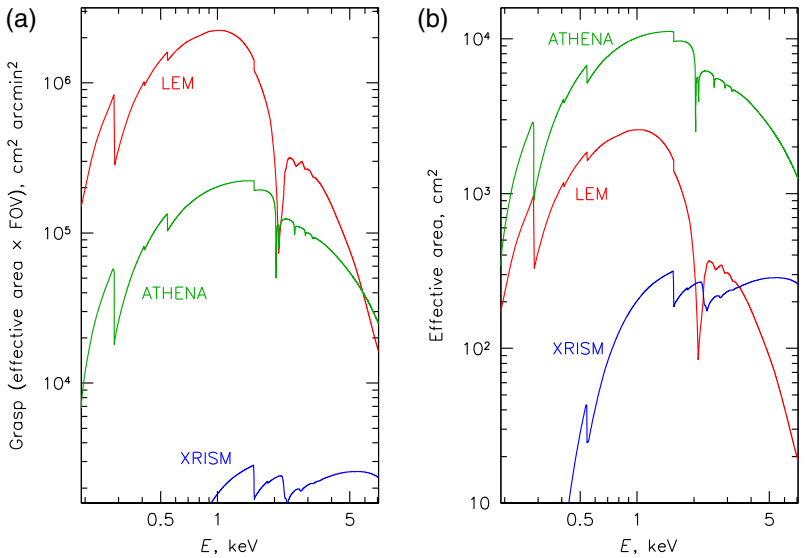

Fig. 3 LEM effective area and grasp—the product of the effective area and the FoV solid angle—compared to XRISM Resolve and the Athena XIFU (prior to 2022 reformulation). Grasp is the quantity relevant for mapping faint extended objects with sizes comparable to or greater than the FoV (such as nearby galaxies, clusters, the IGM, or the Milky Way structures)—for such targets, the number of photons collected in a given exposure is directly proportional to grasp. Figure reproduced with permission from Ref. 8.

of the sky to which LEM will have access at any time of year, the observatory will be responsive to requests to observe astrophysical transients through a robust Target of Opportunity (ToO) program, as well as a robust GO program of targets scattered around the sky.

Ground contacts with LEM are planned for an approximately daily cadence, with 1 hour devoted to data downlink. The typical data rate of 37.1 kbit s^{-1} will accommodate all but the brightest X-ray targets, which are expected to have a rate >5 Mbit s^{-1}. For bright sources, LEM will make use of a suite of optical block filters (OBFs) or neutral density filters (NDFs), to be able to downlink the data within the allotted bandwidth (see Sec. 4.3.2 for more details.) Flight operations for LEM will be conducted by Lockheed–Martin (LM), with science operations provided by the Smithsonian Astrophysical Observatory, in Cambridge, Massachusetts, United States.

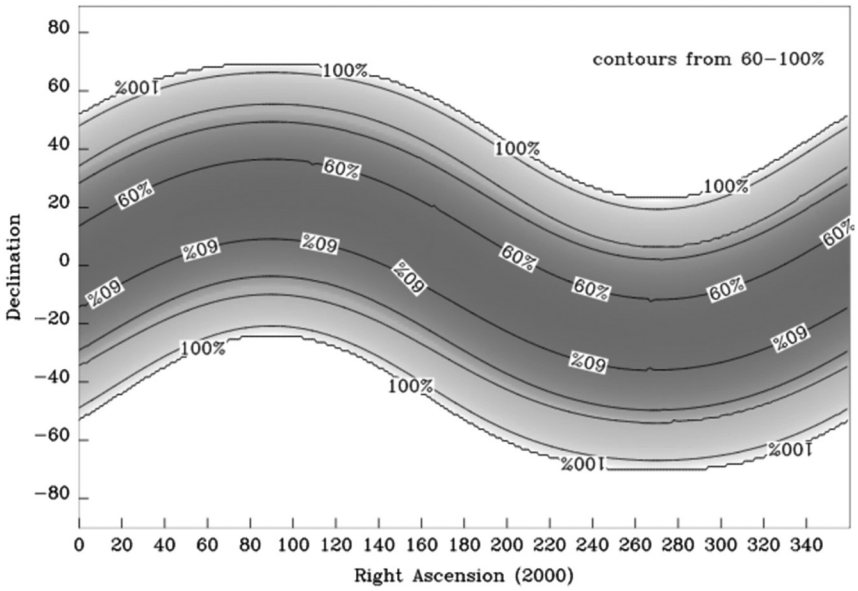

Fig. 4 Average sky visibility for LEM, positioned at L1, with a field of regard between 45 and 150 deg.

LEM will operate in two modes. The first mode consists of pointed observations of directed or GO-proposed science targets. During these pointed observations, LEM will dither with a Lissajous pattern within a $\gtrsim 45'' \times 45''$ box. Dithering the satellite will compensate for any dead pixels in the detector and possibly for sub-pixel image and aspect reconstruction during post processing. This is because the $10''$ HPD of the mirror fills an individual LMS pixel, so dithering across pixel boundaries will allow for more accurate source localization. To complete one full Lissajous pattern, the minimum exposure time for a LEM observation will be expected to be 1000s. The maximum allowable dither rate is $<2.2'' \text{ s}^{-1}$, which will allow for a large range of user-specified dither parameters.

The LEM mission also plans an all-sky survey. This is a slew mode where the satellite will sweep across and uniformly cover large patches of sky, providing an average exposure of 100 sec FoV^{-1}, to a depth of > 1 photon sec^{-1} cm^{-2} steradian^{-1} in specific interesting lines, such as the O VIII triplet. An example spectrum integrated over a 10 deg $\times$10 deg summed patch of sky is shown in the upper panel of Fig. 6. During this mode, the satellite will not dither, as the natural slew of the satellite will aid in minimizing the effects of bad pixels and work to smear out bright X-ray sources. Given the average exposure per FoV, this mode will comprise 16 Ms of exposure time.

3 LEM Science

The LEM design is driven by the Astro2020 decadal survey key questions concerning cosmic ecosystems at all scales, feedback, and the drivers of galaxy growth. Galaxies are governed by gravity and feedback from processes, such as the life cycles of stars and winds, driven by supermassive black holes. Theoretical predictions from simulations for structure formation in the cosmos predict that the history of this feedback is encoded within the CGM, and on larger scales, the IGM, while this feedback is observed in near real time in our own galaxy, by way of supernova remnants (SNRs) and star-forming regions. The result is a circulation of gas and metals (synthesized by stars and supernovae in galaxies) into and out of galaxies—a galactic ecosystem.

At the most local of galactic scales, stellar feedback, by way of the complete lifecycles of stars, chemically enriches the environment and leads to the formation of structure—bubbles, SNRs, and chimneys—that forces energy and material into the Milky Way CGM. With its large grasp, LEM will be able to efficiently map these structures, from pc scale SNRs such as Puppis A, shown in Fig. 5, to kpc scale outflows such as Fermi and eRosita bubbles, shown in Fig. 6.

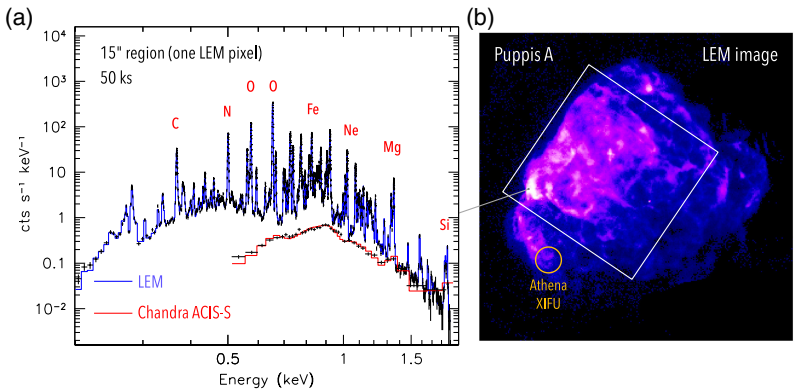

Fig. 5 (b) The galactic SNR Puppis A, with a $30' \times 30'$ LEM FoV overlaid. The Athena X-IFU is shown for comparison. (a) A single LMS pixel spectrum of Puppis A for a simulated 50 ks LEM observation. A Chandra ACIS (CCD resolution) spectrum of the same region of the remnant is shown for comparison. Figure reproduced with permission from Ref. 8.

Moving beyond our local neighborhood, LEM will probe how the gas produced and ejected by stars and SNRs flows into their host galaxy's CGM. LEM will map the CGM (defined here as the gaseous halo within the galaxy virial radius R_{200}, where the virial radius is defined as the radius where the local density is equivalent to the critical density of the universe at the galaxy's redshift) in the emission lines of X-ray bright ions, such as O VII, O VIII, and Fe XVII. The high spectral resolution of the LMS will enable the faint CGM emission to be disentangled from bright galactic foreground emission, as demonstrated in Fig. 7. Current and planned CCD-resolution detectors simply lack the resolution to perform this measurement.

Beyond the confines of galaxy clusters and galaxies lies tenuous, faint IGM with temperatures 10^{5-7} K (formerly "missing baryons," whose presence has now been detected; also known as warm-hot IGM, or WHIM). This is the ultimate repository for all the chemically enriched material expelled from galaxies over their cosmological lifetimes, which makes it invaluable for our understanding of galaxy formation. The existing X-ray instruments cannot study this extremely faint medium beyond the immediate vicinity of massive galaxy clusters. LEM is ideally suited to study the faint IGM—its nondispersive energy resolution will let us see the faint redshifted emission lines from the IGM through the forest of the much brighter Milky Way lines, its large grasp will enable us to collect enough IGM photons within practical exposure times, and its angular resolution will allow us to exclude the point sources of the cosmic X-ray background.

3.1 General Observer Science

While LEM was conceived and designed to map hot gas flows in a wide range of astrophysical environments and answer key questions in the Astro2020 decadal's cosmic ecosystems theme, it will also provide powerful new capabilities to the entire X-ray astrophysics community through a robust GO program. Time domain science and multi-messenger astrophysics are not primary design goals for the LEM mission architecture. However, LEM will have a ToO capability to provide calorimeter resolution spectra providing new insights into a wide range of astrophysical phenomena including tidal disruption events, electromagnetic counterparts to merging black holes, stellar flares, and dwarf novae, among many others.

According to the terms of the APEX announcement of opportunity, at least 70% of the LEM observing time must be allocated to GOs. The GOs can request to use LEM to make science investigations in all areas of astrophysics through a competitive peer review process. We anticipate that LEM will be used to measure the ionization state and velocity of gas ejected from the accretion disk near supermassive black holes, characterize the spectrum of coronally-active stars, measure the flux and duty cycle of X-ray emission from young stars to determine the impact that stellar activity has on planet formation, plus a host of other investigations.

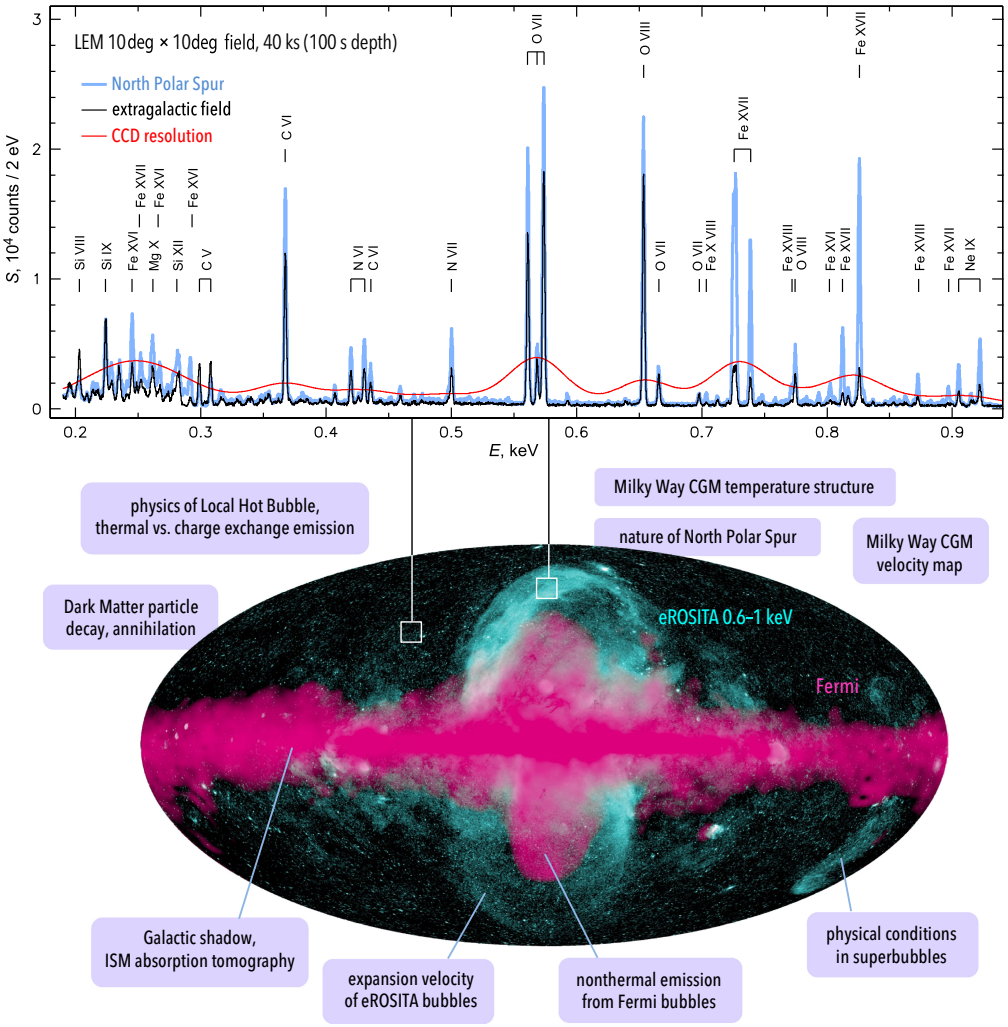

Fig. 6 LEM shallow all-sky survey. The all-sky map[10] in galactic coordinates overlays soft X-ray emission from SRG/eROSITA (cyan) and γ-ray emission from Fermi (magenta). Top: Example simulated spectra for 10 deg $\times$ 10 deg regions (marked by squares) and 100 s depth are shown for an average high-latitude region outside of any bright features ("extragalactic field"), and another for the North Polar Spur; the CXB is included. Purely thermal CIE plasma models are assumed. Red curve shows the NPS spectrum at CCD resolution (e.g., eROSITA). LEM will resolve the forest of lines and gain access to line diagnostics for temperature, nonequilibrium and charge exchange processes. The survey will allow us to map the temperature structure and velocities of the Milky Way inner CGM on few-degree scales—including the expansion of the eROSITA/Fermi bubbles, believed to be produced by the central SMBH or star-forming regions. Numerous other investigations, some of which are labeled in the figure, will become possible. Figure reproduced with permission from Ref. 8.

Additionally, the deep observations of LEM of galaxy haloes and cluster filaments taken as part of the directed portion of the mission will provide a wealth of ancillary science for archival studies by guest investigators. Tens of thousands of AGN will be detected in aggregate in these fields—all with calorimeter resolution spectra. Thousands of stars will be detected in the LEM observations of star forming regions thus providing calorimeter resolution spectra for all coronally active stars. Observations over multiple epochs will provide a unique dataset on both intensity and spectral variability of these stars. LEM will also be used to observe all categories of objects in the Solar system including rocky planet exospheres, gas giant magnetospheres, comets, and the Solar wind interaction with these objects. Finally, LEM will have broad synergies with all the major facilities of the 2030s, including CMB-S4, square kilometer array, Giant Magellan Telescope, Roman Space Telescope, Athena, and many others.

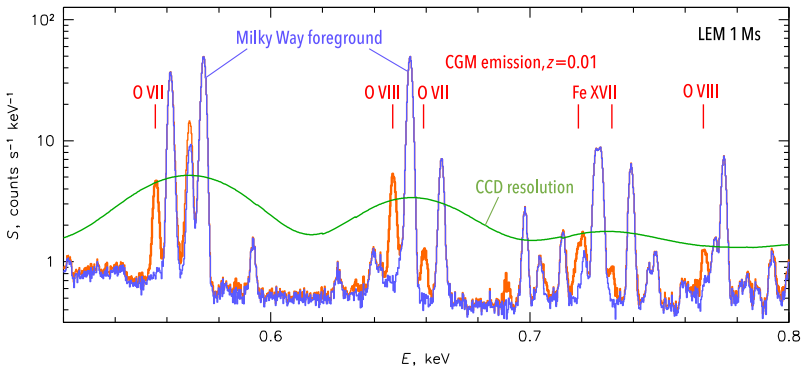

Fig. 7 Simulated LEM spectrum of the CGM of a galaxy twice as massive as the Milky Way (from TNG simulations[11]), at $z = 0.01$ or 40 Mpc, for a 1 Ms exposure and the ~2 eV resolution of the full detector. Blue line shows the spectrum of the foreground, red line includes the CGM signal. The spectrum is extracted from a broad annulus between 0.25 and 0.75 R_{500}. Point sources detected with the LEM angular resolution are excluded. Because the Milky Way emits in the same spectral lines but is over an order of magnitude brighter, it is impossible to disentangle the two with the present CCD instruments, such as Chandra and XMM-Newton (green line). A non-dispersive spectrometer with ~2 eV resolution allows the study of the faint CGM for galaxies at $z \gtrsim 0.01$, where they can also be well-resolved spatially. Figure reproduced with permission from Ref. 8.

4 LEM Science Implementation

The LEM science program requires an instrument with a large effective area coupled to a large FoV and unprecedented non-dispersive energy resolution in the 0.2 to 1.9 keV band. In this section, we describe the LEM instrument, as shown in Fig. 2. Broadly speaking, LEM consists of an X-ray mirror assembly (XMA), which focuses X-rays onto the LEM focal plane assembly (FPA). To minimize particle background, a magnetic diverter (MD) is located within the optical bench assembly (OBA), approximately 1m above the focal plane. A filter wheel is located above the focal plane to facilitate observations of bright optical or X-ray sources and to allow for LMS calibration before opening the gate-valve on the dewar. For in-flight calibration, a modulated X-ray source (MXS) is stationed within the XMA.

4.1 X-Ray Mirror Assembly

The XMA focuses X-rays onto the FPA. Key requirements imposed on the XMA by the science objectives are point-spread-function (PSF), effective area, and FoV. LEM uses the single crystal silicon mirror technology that has been under development at Goddard Space Flight Center for the last decade to achieve the PSF requirement at a much lighter weight and a much larger effective area, with a much lower cost,[12–15] when compared to previous mirror development technology such as what was employed for the Chandra mirrors. The overall XMA optical design is driven by both the PSF and FoV requirements. The XMA adopts a WS type 1 design to provide the best possible on- and off-axis images. A mechanical diagram of the XMA is shown in Fig. 8.

The major components of the XMA are the spider, thermal pre/post-collimators, 150 mirror modules (MMs), an interface ring, and heaters and thermistors. The spider is the structural backbone for the XMA mirrors. It is aluminum and thermally controlled to 20 ± 0.25 C, to maintain the confocality of the 150 MMs. The thermal pre/post-collimators are part of the thermal control hardware. They minimize the view of the MMs to cold space and the cold telescope tube. The 150 MMs are at the heart of the XMA.

Each module is an X-ray telescope in its own right, contributing a part to the XMA effective area. They are each individually aligned and attached to the spider via flexures that isolate the MM structurally and thermally, providing the best possible structurally and thermally stable environments. Each MM consists of a spine made from single crystal silicon that supports the entire module, many mirror segments made of single crystal silicon that are attached to the spine via flexuators (flexure plus actuator); pre/post-thermal baffles; and heaters and thermistors that heat the spine directly and mirror segments indirectly via the pre- and post-thermal baffles.

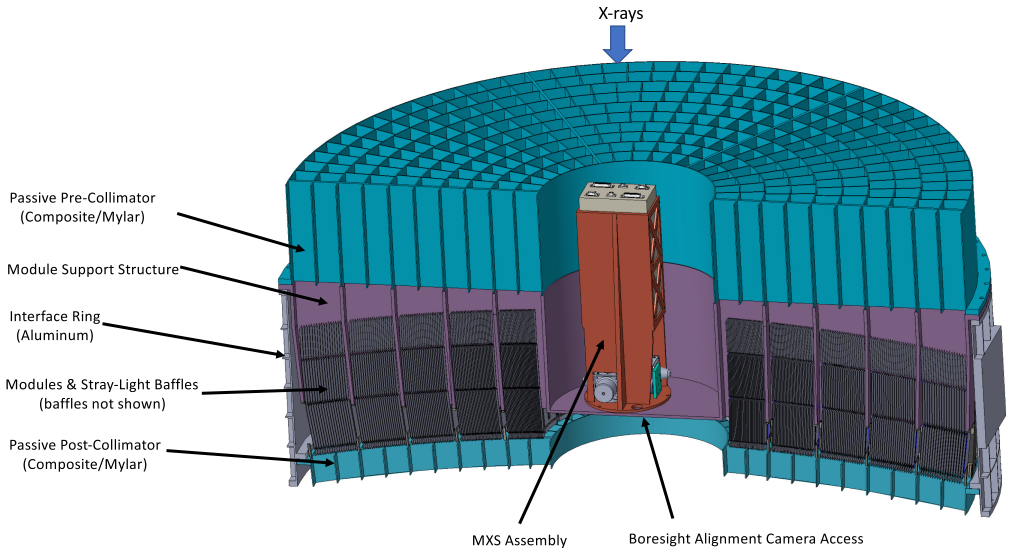

Fig. 8 Schematic view of the LEM XMA. The XMA consists of five concentric rings, for a total of 150 MMs.

The spider assembly and pre/post-collimators integrate to the Al interface ring that provides the structural interface to the telescope tube (OBA) linking the XMA to the LMS. The XMA also has heaters and thermistors to facilitate thermal control. Stray light or stray X-rays (i.e., X-rays that could reach the focal plane without the proper two reflections) are blocked by three implements: the front vanes (stray light baffles), front aperture stop (front annular baffle), and a middle aperture stop (intersection annular baffle).

4.2 Modulated X-Ray Source

The LEM MXS, as shown in Fig. 9, generates characteristic aluminum Kα (1.5 keV) X-rays that are used to correct time-dependent drift in the detector pulse-height-energy relation (detector gain). It can be quickly modulated (up to 10 kHz) to allow efficient interleaving of science data acquisition and gain calibration. All of the components of the MXS and its controller derive from heritage designs and is used in the same manner as the MXS deployed on XRISM/Resolve[16,17] and as is planned for the Athena X-IFU.

The source itself consists of a ultraviolet light emitting diode (LED) illuminating a photocathode, which in turn emits electrons that impact and are amplified by a channel electron multiplier, with the resulting output current pulse being accelerated onto a target anode at high voltage (4 kV), thus generating X-rays. The design of the LEM source and its vacuum/mechanical housing is based on the design of the XCOM MXS, which has been qualified through a full

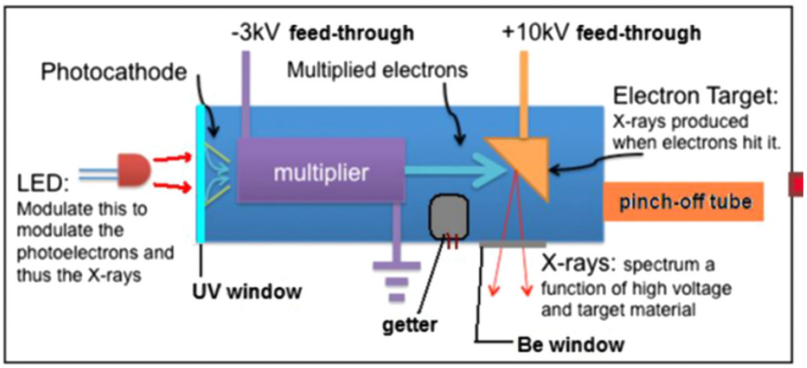

Fig. 9 Preliminary design for LEM MXS based on the XCOM/GEMS heritage design. The MXS consists of a modulated LED, which illuminates a photocathode. Electrons are then fed into an electron multiplier, which impact an aluminum target, producing X-ray photons.

suite of environmental testing. The LEM MXS assembly will include two redundant MXS sources, each paired with its own dedicated controller. The two sources and two controllers will be assembled within a frame structure, which in turn will be installed in the open center of the XMA, allowing unobstructed illumination of the focal plane.

4.3 Optical Bench Assembly

The OBA comprises the primary structure spanning the 4-m distance between the XMA and the Dewar. The two segment conical structure is 135 inch long, 105 inch in diameter at the top, and 32 inch in diameter at the bottom. It is made of 0.1 inch thick M55J/954-3 2×2 twill carbon fiber wrapped in multilayer insulation on the outside. The M55J material has been used extensively by LM Space. Using the M55J and designing to reduce other sources of thermal expansion, the OBA has an expected thermal lateral shift of 3 microns and axial shift of 33 microns, exceeding all stability requirements by three orders of magnitude for all spacecraft thermal conditions.

The cone is split into two segments to ease layup to provide an additional optical baffle for the X-rays and allow for the installation of the MD and filter wheel. The position of these components is not critical, allowing them to be installed with acceptable accuracy at the sub-assembly level. The interface at the top of the cone and the Dewar modal allows for the fine manipulation of the Dewar into the focal path during ground operations, using a boresight camera located in the mirror, prior to permanently attaching the module for launch.

4.3.1 *Magnetic diverter*

The XMA is just as efficient at reflecting soft protons with energies up to several hundred keV as it is at focusing soft X-rays. These soft protons result in a poorly characterized increase in the detector background, as they can interact with the detector and produce secondary charged particles. For Athena, this particle background is anticipated to comprise ~10% of the total background, or $\leq 5.5 \times 10^{-4}$ cts s^{-1} cm^{-2} keV^{-1}.[18] To aid in reducing this increased background, a MD is placed within the upper section of the OBA. It acts to sweep the primary high-energy protons out of the optical path. The diverter design, as shown in Fig. 10, is based on a similar application for the Athena X-IFU and WFI instruments, which uses a Hallbach design comprised of N42H grade BREMAG NdFeB magnets.[18]

The LEM MD consists of a ring of these magnets with a 38 cm inner diameter placed ~1 m from the detector. The magnet housing uses an aluminum ring machined with pockets to contain the individual block magnets, which are held in place with covers for each pocket around the outer diameter. The MD contains 22 NdFeB magnet blocks, each $\sim 6 \times 7 \times 6.4$ cm separated by 4 mm fins. The MD is integrated into an internal deck within the upper section of the OBA just below the operating envelope of the filter wheel assembly (FWA).

4.3.2 *Filter wheel assembly*

Located between the MD and the outer thermal filter on the LMS dewar is the FWA. The FWA is designed and built as a collaoration between the Smithsonian Astrophysical Observatory, University of Geneva, and Goddard Space Flight Center. Filters for X-ray and optically bright sources have flown previously on XMM-Newton, Hitomi and are included in XRISM.[17,19]

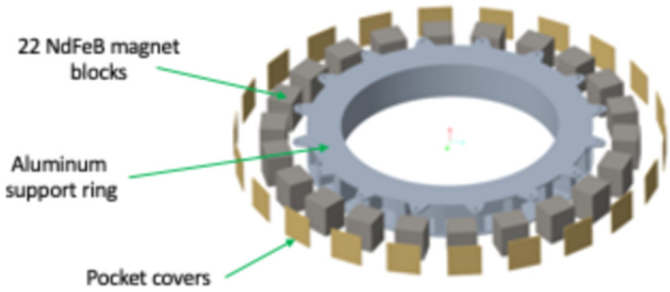

Fig. 10 Notional design for LEM MD.

The LEM FWA will consist of seven filter positions. There will be an open position, which will be used for >90% of all science observations, and a closed position for use during satellite saving actions. To facilitate observations of astrophysical sources where optical loading on the focal plane is a concern, two optical blocking filters, consisting of aluminized polyimide, will be available. For bright or very bright X-ray sources, NDFs, comprised of molybdenum drilled with holes will be available, notionally providing 1% or 50% throughput. Finally, the seventh position will contain a ^{55}Fe source. This radioactive source will allow for LMS checkout ahead of opening the gate valve on the dewar.

4.4 LEM X-Ray Microcalorimeter Spectrometer

The LEM microcalorimeter spectrometer (LMS), as shown in Fig. 11, is a cryogenic instrument with a focal plane microcalorimeter array that has been designed to leverage the large amount of investment and research into cryogenic and microcalorimeter instrumentation as well as mission development over the past two decades, to produce a mature, reliable, and high-heritage design. It is based upon the use of a large-format TES microcalorimeter array, read out using time-division multiplexing (TDM). The overall LMS architecture is shown in Fig. 11. The LMS consists of a vacuum Dewar, with a single pulse-tube to cool the core of this instrument down to 4 K, and a continuous adiabatic demagnetization refrigerator that continuously cools the microcalorimeter to 40 mK inside an FPA. An aperture assembly inside the Dewar, behind a gate valve that opens in orbit, allows X-rays concentrated by the X-ray optic to pass through to the detector, while also acting as thermal blocking filters to minimize optical and IR radiation on the focal plane.

The architecture is largely based upon that developed for Astro-E,[20] Astro-E-2,[21] Hitomi, and XRISM.[17] This has been updated to include the detection chain and FPA needed to read out a large array of TESs using TDM. A core part of the Athena X-IFU team consists of LMS scientists and engineers, as LMS team members are providing similar detectors and the same type of multiplexed read-out (SQUID TDM) as is baselined for the LMS, on behalf of NASA. The detection chain architecture has flight heritage from the two sounding rocket flights of Micro-X.[22–24] The overall mass is estimated to be 368 kg, including the main cryostat, electronics boxes, and all the additional thermal and structural components of the LMS connected to the optical bench. This mass is more than six times less than the Athena science instrument module prior to reformulation. Details on the individual components of the LMS are discussed in detail elsewhere in this JATIS special section.[2–7]

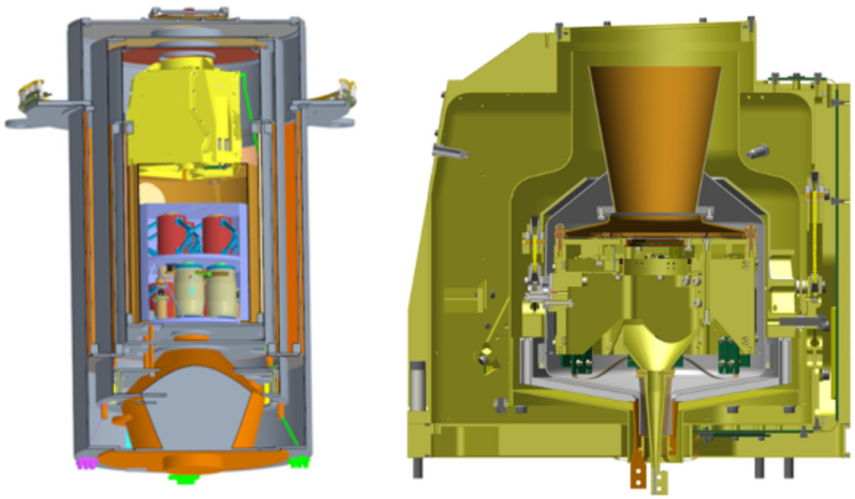

Fig. 11 (a) LEM microcalorimeter spectrometer, showing the three concentric aluminum shells, consisting of one vacuum shell and two radiation shells at 18 and 100K.[6] (b) LEM FPA mechanical housing and detector.[2] In both drawings, X-rays enter from the top.

5 Summary

To achieve the breakthrough scientific objectives of LEM, we have designed a high-throughput, high-resolution imaging X-ray spectrometer, or IFU, which has been optimized to meet the mission scientific requirements by applying the results of nearly three decades of research and development in X-ray calorimeters and X-ray optics. Based on this extensive work, the array and mirror designs can be tailored to a broad range of scientific goals.

The primary LEM design goal is to obtain high-contrast images in the prominent X-ray line features of circumgalactic and cosmic web structures. This requires both a high effective area and a large FoV, due to the low surface brightness of these large and diffuse objects, combined with sufficiently high spectral resolution to cleanly separate the emission from the red-shifted target galaxies from the similar foreground emission features of the Milky Way. With its large FoV, low background, and high throughput and spectral resolution, LEM is optimized to efficiently address this need.

LEM will provide a paradigm-shift in capabilities compared to the current generation of X-ray observatories by combining high spectral resolution with wide-field imaging instrument. This mission is scientifically compelling with capabilities that span all of X-ray astrophysics, implementable at the $1B APEX price cap and highly relevant to the astrophysics landscape of the 2030s. LEM would truly take our field into new and exciting directions should it be selected as the first in this line of new NASA missions.

Code and Data Availability

There are no data or software associated with this manuscript.

Acknowledgments

D. Patnaude, A. Bogdan, J. Drake, C. Garraffo, P. Plucinsky, and J. ZuHone acknowledge support from the Chandra X-ray Center, which is operated by the Smithsonian Institution under NASA (Grant No. NAS8-03060). A. Orgozalek acknowledges that this material is based upon work supported by NASA (Grant No. 80GSFC21M0002). The authors wish to thank the reviewers for the many thoughtful comments and questions, which aided in the development of this manuscript.

References

1. National Academies of Sciences, Engineering, and Medicine, *Pathways to Discovery in Astronomy and Astrophysics for the 2020s* (2021).
2. S. Bandler, "The Line Emission Mapper microcalorimeter spectrometer," *J. Astron. Telesc. Instrum. Syst.* **9**, 041002 (2023).
3. A. Jahromi, "The compact and efficient continuous adiabatic demagnetization refrigerator for LEM," *J. Astron. Telesc. Instrum. Syst.* **9**, 041003 (2023).
4. S. Smith, "Development of the microcalorimeter and anti-coincidence detector for the Line Emission Mapper X-ray Probe," *J. Astron. Telesc. Instrum. Syst.* **9**, 041005 (2023).
5. N. Wakeham, "Characterization of a hybrid array of single and multi-absorber transition-edge sensor microcalorimeters for the Line Emission Mapper," *J. Astron. Telesc. Instrum. Syst.* **9**, 041006 (2023).
6. E. Osborne, "Line Emission Mapper cryogenic system design," *J. Astron. Telesc. Instrum. Syst.* **9**(4), 041007 (2023).
7. K. Sakai, "Development of space-flight room-temperature electronics for the LEM Microcalorimeter Spectrometer," *J. Astron. Telesc. Instrum. Syst.* **9**, 041004 (2023).
8. R. Kraft et al., "Line Emission Mapper (LEM): probing the physics of cosmic ecosystems," arXiv:2211.09827 (2022).
9. M. Laurenza et al., "Estimation of the particle radiation environment at the L1 point and in near-earth space," *Astrophys. J.* **873**, 112 (2019).
10. P. Predehl et al., "Detection of large-scale X-ray bubbles in the Milky Way halo," *Nature* **588**, 227–231 (2020).
11. D. Nelson et al., "The illustristng simulations: public data release," *Comput. Astrophys. Cosmol.* **6**, 2 (2019).
12. W. W. Zhang et al., "Lightweight and high-resolution single crystal silicon optics for x-ray astronomy," *Proc. SPIE* **9905**, 99051S (2016).
13. W. W. Zhang et al., "Monocrystalline silicon and the meta-shell approach to building x-ray astronomical optics," *Proc. SPIE* **10399**, 103990S (2017).

14. W. W. Zhang et al., "Astronomical x-ray optics using mono-crystalline silicon: high resolution, light weight, and low cost," *Proc. SPIE* **10699**, 106990O (2018).
15. W. W. Zhang, "Silicon meta-shell X-ray optics for astronomy," in *The WSPC Handbook of Astronomical Instrumentation, Volume 4: X-Ray Astronomical Instrumentation*, D. N. Burrows, Ed., pp. 47–62, World Scientific (2021).
16. T. Omama et al., "Relative timing calibration of the Resolve x-ray microcalorimeter onboard XRISM using the modulated x-ray source," *Proc. SPIE* **12181**, 1218162 (2022).
17. K. Sato, Y. Uchida, and K. Ishikawa, "Hitomi/XRISM micro-calorimeter," arXiv:2303.01642 (2023).
18. I. Ferreira et al., "Design of the charged particle diverter for the ATHENA mission," *Proc. SPIE* **10699**, 106994A (2018).
19. C. P. de Vries et al., "Calibration sources and filters of the soft x-ray spectrometer instrument on the Hitomi spacecraft," *J. Astron. Telesc. Instrum. Syst.* **4**, 011204 (2018).
20. R. L. Kelley et al., "The microcalorimeter spectrometer on the ASTRO-E X-ray observatory," *Nucl. Instrum. Methods Phys. Res. A* **444**, 170–174 (2000).
21. F. S. Porter et al., "The Astro-E2 X-ray spectrometer/EBIT microcalorimeter x-ray spectrometer," *Rev. Sci. Instrum.* **75**, 3772–3774 (2004).
22. D. Vaccaro et al., "Susceptibility Study of TES Micro-calorimeters for X-ray spectroscopy under FDM readout," *J. Low Temp. Phys.* **209**, 562–569 (2022).
23. J. S. Adams et al., "Modeling a three-stage SQUID system in space with the first micro-X sounding rocket flight," *J. Low Temp. Phys.* **209**, 702–709 (2022).
24. J. S. Adams et al., "Micro-X sounding rocket payload re-flight progress," *J. Low Temp. Phys.* **209**(5-6), 832–838 (2022).

Daniel J. Patnaude is an astrophysicist at the Smithsonian Astrophysical Observatory. He is the operations scientist for the Chandra High Resolution Camera. He performs observational and theoretical studies of supernovae and supernova remnants. He received his PhD in physics and astronomy from Dartmouth College in 2005 and his BS degree in astronomy from The University of Massachusetts at Amherst in 1995.

Biographies of the authors are not available.